Tinospora cordifolia (Willd.) Hook. f. and Thoms. and Arabinogalactan exert chemopreventive action during B(a)P induced pulmonary carcinogenesis: Studies on ultrastructural, molecular and biochemical alterations

Vandana Mohan & Ashwani Koul*

Department of Biophysics, Basic Medical Science Block II, South Campus, Panjab University, Chandigarh, India

Tinospora cordifolia (Willd.) Hook. f. and Thoms. (Tc) is a medicinal plant gaining considerable attention owing to its wide range of pharmacological properties. Though there are ample reports which have documented its biological activity in various clinical disorders, there is a paucity of information regarding its anticancer activity particularly against B(a)P induced lung cancer. So, the present study evaluates the chemopreventive potentials of aqueous extract of Tc (Aq.Tc) and its active component; Arabinogalactan (AG) against Benzo(a)pyrene [B(a)P] induced pulmonary carcinogenesis in BALB/c mice. B(a)P resulted in significant alteration in carcinogen metabolizing enzymes (CME's), reduced glutathione and lipid peroxidation levels. B(a)P also inflicted clastogenic damage, disturbed phospholipid saturation, protein secondary structures and glycogen content. Altogether these events resulted in the alterations in cellular arrangement of pulmonary tissue, depicting the outburst of lung carcinogenesis. However, Aq.Tc and AG significantly helped to normalize the disturbed levels of CME's and antioxidant machinery. Clastogenic changes, phospholipid saturation, protein secondary structures and glycogen content were also alleviated with Aq.Tc and AG administration. Additionally, B(a)P+ Aq.Tc and B(a)P + AG treated groups revealed the classical features of apoptosis. The results suggest that the aquatic extract of gudichi (Aq.Tc) and Arabinogalactan (AG) modulate various key processes associated with carcinogenesis and can be used as effective chemopreventive agents.

Keywords: Carcinogen metabolizing enzymes, Chromosomal aberration, Giloy, Guduchi, Micronucleus, Oxidative stress

Lung cancer (LC) is one of the most wide spread cancer types as well as the leading cause of death worldwide[1]. The incidence of LC still remains to be very high (2,207 million), as the consumption of cigarettes continues to grow each year[2]. It has claimed approximately 1.8 million lives in 2020[1]. Among the different constituents of tobacco smoke, Benzo(a)pyrene [B(a)P] plays a major role in lung carcinogenesis. It is one of the most potent environmental carcinogens. B(a)P is a pro-carcinogen, which requires metabolic activation to electrophilic reactive metabolites for its carcinogenic activity. After sequential metabolic activation of B(a)P by phase I and II carcinogen metabolising enzymes (CME's), it generates 7,8-diol-9,10-epoxide-benzo(a)pyrene (BPDE) which is capable to bind covalently to DNA and form DNA adducts[3]. BPDE is highly carcinogenic and mutagenic leading to the induction of chromosomal alterations. These genetic changes may further contribute to the initiation of carcinogenesis[4]. Carcinogenesis is well-known to alter the distribution of major cellular components present in biological tissues *viz*., proteins, lipids, nucleic acids and carbohydrates[5]. Alterations in these biomolecules are the result of modified rates of metabolic activity, cellular proliferation and cell death. The changes in structural proteins also play decisive roles in the progression and development of cancer[6]. Therefore, the quantification of these biomolecules during carcinogenesis may pave a new way to understand the mechanism behind its occurrence and its attenuation by various chemopreventive/therapeutic agents.

Cancer chemoprevention with natural phytochemical compounds or extracts is an emerging strategy to prevent, impede, delay, or cure cancer. Therefore, efforts are being made to search for effective chemopreventive agents that can improve the efficacy of cancer treatments or delay the carcinogenesis at various stages. *Tinospora cordifolia* (Willd.) Hook. f. and Thoms. (Tc) (Menispermaceae) commonly known as Giloy/Guduchi is one such medicinal plant which is widely distributed throughout tropical and subtropical regions of Indian subcontinent

*Correspondence:
E-Mail: drashwanikoul@yahoo.co.in, ashwanik@pu.ac.in

and China. It possesses various pharmacological properties including immunomodulatory and anticancer activities especially against epithelial cancer cell types[7]. It has been well documented in the literature that the polysaccharide (PS) fraction from Tc is effective in mitigating the metastatic potential of B16F-10 melanoma cells[8]. One of the primary active PS present in Tc is Arabinogalactan (AG). It has been reported earlier that AG is present in adequate amount in the aqueous PS fraction of Tc and exhibits anticancer activity against various cancer types[9]. Earlier studies conducted in our laboratory investigated the chemopreventive potential of aqueous Tc stem extract (Aq.Tc) and its bioactive PS (AG) against pulmonary carcinogenesis. The results showed a promising anticancer activity in terms of various tumor biomarkers, histopathological alterations and cell death[10]. However, to establish the chemopreventive efficacy of any chemopreventive agent, a complete mechanistic study is needed. Therefore, we planned the present study in continuation of the previous work exploring the chemopreventive mechanism of Tc and its active component AG revealing its potential in modulating various biomolecular and ultrastructural changes induced by B(a)P. A comprehensive study exploring the underlying mechanisms could strengthen its use as a chemopreventive agent.

Material and Methods

Chemicals and Reagents

Benzo(a)pyrene [B(a)P], Uridinediphosphate glucuronic acid (UDP-GA), digitonin, glutaraldehyde, paraformaldehyde and Arabinogalactan (99% pure) were obtained from Sigma-Aldrich Co. (St. Louis, MO, USA). Bovine serum albumin (BSA), 5,5-dithiobis-2-nitrobenzoic acid (DTNB), 1-chloro-2,4-dinitrobenzene (CDNB), thiobarbituric acid (TBA), reduced nicotinamide adenine dinucleotide phosphate (NADPH), nicotinamide adenine dinucleotide (NADH) were purchased from local reputed firms (Sisco Research Laboratory Pvt. Ltd, Central Drug House Pvt. Ltd.) and were of analytically pure grade.

Plant collection, identification and extract preparation

The stems of Tc were collected from the Panjab University Botanical Garden and were identified and authenticated by a qualified Botanist from Department of Botany, Panjab University, India. The lyophilized form of aqueous Tc stem extract (Aq.Tc) was prepared according to the standardized method[10]. Briefly, the collected stems were washed in sterile double distilled water and shade dried. The dried stems were finely grounded in a mixer and sieved to obtain fine powder. 500 mL distilled water was added to 100 g of dried powder of Tc stem in a flask and mixed well. The mixture was briefly vortexed and the slurry thus obtained was filtered. The filtrate was centrifuged at 8000 xg to obtain a clear solution (supernatant). The solution was lyophilized to form a fine powder and stored in a dark container at 4°C for further use. Characterization of the Aq.Tc extract performed in our laboratory revealed the presence of tannins, flavonoids, polysaccharides, carbohydrates and proteins. Also, Aq.Tc extract and AG showed concentration-dependent *in vitro* free radical scavenging activity as depicted by various *in vitro* free radical scavenging assays done previously[10].

Elemental analysis of Aq.Tc extract

The elemental composition of Aq.Tc extract was determined using Wavelength Dispersive X-ray fluorescence WD-XRF (Bruker S4 Tiger, Germany). Aq.Tc extract was dried at 58-60°C for 24 h and powdered to pass a No. 180 sieve. All the instructions were followed according to the guidelines of the World Health Organisation (WHO) for quality control of medicinal plant materials. Samples were stored in an oven at 60°C prior to pelletization. Following recommendations and details from literature, a powder pellet was prepared by mixing 4 g of plant powder with 0.4 g of hoechst cridust wax and homogenising the mixture by using pestle and mortar. The pellets were pressed at 10 t for 120 s to obtain a cylindrical pellet (thickness 2 mm, diameter 34 mm). Samples were analysed using WD-XRF spectrometer equipped with a Rh anticathode x-ray tube (4 kw). The spectra recorded was evaluated using the software (spectra plus) linked to the equipment.

Animals and Experimental conditions

Male BALB/c mice (25-30 g) were procured from Central Animal House, Panjab University, Chandigarh, India (Approval no PU/IAEC/S/15/61). The animals were housed in polypropylene cages bedded with sterilized rice husk and were provided with standard pellet diet and water *ad libitum*. Animals were kept in standard conditions of temperature (24±2°C), relative humidity (50-60%) and with a 12 h dark and light cycle. Animals were first acclimatized to the experimental conditions for one week after which various treatments were given. All experimental protocols were permitted by the

Institutional Ethics Committee (Panjab University, Chandigarh) and were performed adhering to the doctrine of Indian National Science Academy.

Experimental model

Mice were randomly segregated into 6 groups (n=8 each). Group I animals served as control. The amount of same vehicle (water) was given to the control animals. Group II animals were administered with Aq.Tc (200 mg/kg body wt., orally) on alternate days for 22 weeks. Group III animals were administered with AG (7.5 mg/kg body wt., orally) on alternate days for 22 weeks. Group IV animals were treated with B(a)P (50 mg/kg body wt., *i.p.*) at 2nd and 4th week of the treatment. The vehicle chosen for both Aq.Tc and AG dose administration was distilled water. Group V animals received Aq. Tc and B(a)P as per the protocol defined for Gr. II and IV, respectively. Group VI animals received AG and B(a)P as mentioned for Gr. III and IV, respectively. Dose and route of B(a)P, Aq.Tc and AG was standardized in our laboratory previously[10,11]. Dose of AG was chosen by calculating the amount of AG present in 200 mg of Aq.Tc (Dubois phenol sulphuric acid method) which amounts to 7.5 mg. The body wt., diet and water intake were observed on weekly basis.

Tumor formation

The extent of tumor formation and the type of tumor formed (in terms of histopathology) has been published earlier[10].

Sample preparation for biochemical estimations

In order to investigate the response of Aq.Tc and AG on the extent of oxidative stress and the status of CME's during pulmonary carcinogenesis, the animals were sacrificed by decapitation at the end of 2nd, 10th and 22nd weeks, respectively. At each time point, biochemical estimations were performed in 6 animals from each group.

Pulmonary tissue was excised and perfused with ice cold normal saline (0.9% NaCl solution), blot dried, and then weighed carefully. 25% (w/v) homogenate was prepared in 100 mM potassium phosphate buffer (pH 7.4) containing 150 mM KC1. It was further subjected to cold centrifugation at 10,000×g for 30 min and the supernatant obtained was stored at 4°C for estimation of cytochrome P_{450} (Cyt P_{450}), cytochrome b_5 (Cyt b_5), aryl hydrocarbon hydroxylase (AHH) and UDP-glucouranosyl-transferase(UDP-GT). Remaining homogenate was diluted with Tris buffer to obtain 10% homogenate (w/v). Aliquots of 10% homogenate were also kept at

4°C for estimation of reduced glutathione (GSH) levels. The remaining homogenate was subjected to cold centrifugation at 10,000×g for 30 min and the supernatant (post-mitochondrial fraction) obtained was used for estimation of lipid peroxidation (LPO) levels and Glutathione-S-transferase (GST) activity.

Phase I carcinogen metabolising enzymes

Cytochrome P_{450}

Cyt P_{450} activity was determined according to the method of Rajakumar *et al.*[12]. The activity of Cyt P_{450} was expressed in nmole/mg protein.

Cytochrome b_5

Cyt b_5 activity was determined by recording the difference spectrum of NADH reduced versus air saturated samples by the method of Koul *et al.*[13]. Activity of Cyt b_5 was expressed in nmole/mg protein.

Aryl Hydrocarbon Hydroxylase (AHH)

The activity of AHH in microsomal preparation was estimated according to the method of Nebert & Gilboin[14]. The activity of AHH was measured using a spectrofluorimeter at an excitation wavelength of 396 nm and an emission wavelength of 522 nm. Solution of 3-hydroxy-B(a)P was used as a standard for calculating the activity of AHH. The activity of AHH was expressed as pmole of 3-hydroxy-B(a)P generated/min/mg protein.

Phase II carcinogen metabolising enzymes

Glutathione-S-transferase (GST)

GST activity was determined according to the method of Devadoss *et al.*[15]. The specific activity of GST was expressed as μmole of GSH-CDNB conjugates formed/min/mg protein.

UDP-Glucouranosyl-transferase (UDP-GT)

The activity of UDP-GT was estimated by the method of Gorski & Kasper[16]. The decrease in absorbance due to formation of UDP-glucuronic acid-p-nitrophenol conjugates was recorded on spectrophotometer at 440 nm. A standard curve was prepared using different concentrations of p-nitrophenol for the calculation of UDP-GT activity. The activity of UDP-GT was expressed as μmole of p-nitrophenol-UDP-glucuronic acid conjugates generated/min/mg protein.

Extent of oxidative stress

Reduced Glutathione (GSH)

GSH was estimated as the total non-protein sulphydryl group by the method described by Moron

et al.[17]. The absorbance was read at 412 nm. GSH was used as a standard to calculate the amount of GSH which was expressed as nmole of GSH/mg protein.

Lipid peroxidation (*LPO*)

NADPH dependent lipid peroxidation was estimated as described by Trush *et al.*[18]. The MDA-TBA chromophore concentration was measured at 535 nm and expressed as nmole MDA formed/min/mg protein.

Protein estimation

Protein estimation of the samples was performed by the method of Lowry *et al.*[19] using BSA as a standard.

Clastogenic damage

Chromosomal aberrations

Chromosomal aberration assay was performed as described by Bala *et al.*[20]. The animals were injected with colchicine (8 mg/kg of body wt.), 12 h prior sacrifice. Mice were dissected and cells were isolated from lung tissue. The cells were incubated with 0.56% (w/v) KCl solution at 37°C for 12 h. After incubation, the cells were centrifuged at 500×g for 10 min. The pellet thus obtained was re-suspended in cornoy's fixative and the suspension was dropped on the tilted ice cold slides (angle 40˚) from a height of about 60 cm. The slides were then flame dried for few seconds. The slides were stained with 5% Giemsa stain solution. A total of 100 slides (single cell chromosomes per animal in each group) were analysed for chromosomal aberration at a magnification of 100X under light microscope. The chromosomal aberrations were classified as mild pulverization (5-10 chromosomal fragments), moderate pulverization (10-20 chromosomal fragments) and extensive pulverization (more than 20 chromosomal fragments).

Micronucleus assay

Micronucleus assay was performed by the method of Schmid[21]. Briefly, lung tissue was homogenized in homogenizing buffer and was then centrifuged at 6000×g for 10 min. The pellet thus obtained was re-suspended in homogenizing buffer. This suspension was used to prepare smears of cells over glass slides and air dried. The slides were then stained using May-Grunwald and Giemsa stain. After staining, slides were mounted with DPX and examined under light microscope for micronuclei (MN) counting.

Fourier Transform Infra-red spectroscopy (FT-IR)

Sample Preparation for FT-IR spectroscopy

Lung tissues were removed after perfusion with ice-cold normal saline. The tissue was grounded using liquid nitrogen and freeze drying was performed to remove excess water. For FT-IR measurements, the powdered sample was mixed with KBr and then made into pellets of 1.2 cm diameter using hand hydraulic press (Perkin Elmer, Germany). The pellets thus obtained were used in FT-IR spectrometer for measurement.

Data acquisition

FT-IR spectra were obtained in the transmission mode with FT-IR spectrometer. The spectra were obtained in Mid-IR region ranging from (400-4000) cm^{-1}. 64 interferograms were recorded and averaged at a spectral resolution of 2 cm^{-1} for each spectrum (sampling interval 1.0 cm^{-1}). Data was corrected with background energy reading (percentage transmittance) from blank KBr pellet. Each spectrum was baselined using polynomial function and then normalized to adjust optical characteristics of each sample.

FT-IR spectroscopic analysis

The spectral data was analysed in two ways. The ratio of various characteristic bands was analysed by integrating each absorption band using FT-IR software. Before integration, spectra were normalized for peak at 1536 cm^{-1} (Amide II). Following normalization, band area ratio was obtained for analysis. Assignments were taken from Lewis *et al.*[22].

Ultrastructural investigations

Scanning electron microscopy (SEM)

The lung tissue was fixed in 4% glutaraldehyde solution prepared in 200 mmol/L phosphate buffer (pH 7.2) for 2 h. Critical point drying was performed to remove any traces of water. Sections were placed inside sputter coater for gold coating. These sections were then examined under LEO 435 VP scanning electron microscope at All India Institute of Medical Sciences (AIIMS, New Delhi, India).

Transmission electron microscopy (TEM)

Lung tissue from different treatment groups were fixed for 2h in 4% glutaraldehyde solution prepared in 0.2M phosphate buffer (pH 7.2) and post fixed in 1% cacodylate buffer (pH 7.2) for 3 h. Ultrathin sections were cut using Leica Ultracut (UCT) microtome.

These sections were mounted on colloidon carbon coated grids and examined with electron microscope (Philips CM-10) at AIIMS, New Delhi, India.

Statistical analysis

The experimental data are represented as Mean ± SD. The data was analysed using one way analysis of variance (ANOVA) test followed by least significant difference (LSD), post hoc test by using Software Package for the Social Sciences (SPSS) version 16 (SPSS Inc. Chicago. IC.)

Results

Elemental Analysis of Aq.Tc extract

The quantitative analysis of various elements in Aq.Tc extract revealed that K, Ca, Si, Mg, P, and S are present in considerable amounts. However, Rb, Zr and As are amongst the elements that were in least amount (Table 1).

Tumor formation

Histopathological analysis of lung tissue revealed tumor formation in B(a)P, B(a)P + Aq.Tc and B(a)P + AG group at 22nd week of the treatment. However, the number of tumors and extent of tumor formation was less in B(a)P + Aq.Tc and B(a)P + AG group (Fig. S1All supplementary data are available only online along with the respective paper at NOPR repository at http://nopr.res.in). The tumors formed in lung tissue in B(a)P group were classified as adenocarcinomas on the basis of histopathological findings/characteristics. Histopathological analysis showed increased hyperproliferation in alveolar region of lung tissue from B(a)P group accompanied by presence of hyperchromatic nuclei. However in B(a)P + Aq.Tc

Table 1 — Trace element analysis of aqueous *Tinospora cordifolia* stem extract

Element	Concentration (ppm)	%
K	20100	2.01
Ca	13400	1.34
Si	6000	0.60
Mg	3500	0.35
P	3100	0.31
S	2500	0.25
Al	1900	0.19
Cl	1500	0.15
Fe	1300	0.13
Na	700	0.07
Ti	200	0.02
Re	68	0.0068
Sr	50	0.0050
Rb	13	0.0013
As	12	0.0012
Zr	8	0.0008

and B(a)P + AG group decreased number of hyper-chromatic irregular cells was evident.

Phase I carcinogen metabolising enzymes

Cytochrome P$_{450}$

After 10th week of the study, significant increase in the activity of Cyt P$_{450}$ was observed in B(a)P group in comparison to control ($P \leq 0.01$), Aq.Tc ($P \leq 0.01$) and AG (p≤0.001) group respectively. B(a)P+AG and B(a)P+ Aq.Tc group showed significant decrease in the activity of Cyt P$_{450}$ in pulmonary tissue in comparison to the B(a)P *($P \leq 0.01$)* group. At 22nd week of the treatment, B(a)P treatment resulted in significant increase in Cyt P$_{450}$ activity as compared to control ($P \leq 0.001$) and AG group ($P \leq 0.001$), whereas, co-administration of AG and Aq.Tc to B(a)P group animals significantly helped to decrease the Cyt P$_{450}$ activity in comparison to B(a)P group ($P \leq 0.01$) (Table 2).

Cytochrome b$_5$

After 10th week of the study, significant increase in the activity of Cyt b$_5$ was observed in B(a)P group when compared to control ($P \leq 0.01$), Aq.Tc ($P \leq 0.01$) and AG ($P \leq 0.001$) group, respectively. B(a)P+AG and B(a)P+ Aq.Tc group animals showed significant decrease in the activity of Cyt b$_5$ in comparison to the B(a)P ($P \leq 0.01$) group. Similarly, at 22nd week, B(a)P treatment resulted in significant increase in Cyt b$_5$ activity as compared to control ($P \leq 0.001$) and AG group ($P \leq 0.001$), whereas, co-administration of AG and Aq.Tc to B(a)P group animals significantly helped to decrease the Cyt b$_5$ activity in comparison to B(a)P group ($P \leq 0.01$) (Table 2).

Aryl hydrocarbon hydroxylase

After 10th week of the study, significant increase in the activity of AHH was observed in B(a)P treated animals in comparison to control ($P \leq 0.01$), Aq.Tc ($P \leq 0.01$) and AG ($P \leq 0.001$) group respectively. B(a)P+AG and B(a)P+ Aq.Tc group animals showed significant decrease in the AHH activity in comparison to the B(a)P ($P \leq 0.01$) group. Similarly, at 22nd week, B(a)P treatment resulted in significant increase in the AHH activity as compared to control ($P \leq 0.001$) and AG group ($P \leq 0.001$), whereas, co-administration of AG and Aq.Tc to B(a)P group animals significantly decreased the AHH activity in comparison to B(a)P group ($P \leq 0.01$). The AHH activity was significantly lower in B(a)P+AG group when compared to the B(a)P +Aq.Tc ($P \leq 0.001$) group (Table 2).

Table 2 — Modulatory effect of Aq.Tc, AG and/or B(a)P on Phase I and II carcinogen metabolising enzymes in pulmonary tissue at 2nd, 10th and 22nd week during lung carcinogenesis

Cyt P_{450} (nmole/mg protein)			
Group	2nd week	10th week	22nd week
Control	0.213±0.018	0.234±0.021	0.239±0.027
Aq.Tc	0.212±0.010	0.218±0.031	0.268±0.036
AG	0.223±0.008	0.220±0.032	0.221±0.033
B(a)P	-	$0.398{\pm}0.035^{a_1 b_1 c_1}$	$0.472{\pm}0.035^{a_1 b_1 c_1}$
B(a)P +Aq.Tc	-	$0.286{\pm}0.035^{d_1}$	$0.215{\pm}0.036^{d_1}$
B(a)P+AG	-	$0.234{\pm}0.040^{d_1}$	$0.231{\pm}0.041^{d_1}$

Cyt b_5 (nmole/mg protein)			
Group	2nd week	10th week	22nd week
Control	0.029±0.003	0.031±0.004	0.031±0.009
Aq.Tc	0.028±0.008	0.026±0.004	0.023±0.008
AG	0.028±0.003	0.028±0.001	0.022±0.006
B(a)P	-	$0.034{\pm}0.003^{a_1 b_1 c_1}$	$0.044{\pm}0.003^{a_3 b_2 c_1}$
B(a)P +Aq.Tc	-	$0.029{\pm}0.003^{d_1}$	$0.031{\pm}0.005^{d_2}$
B(a)P+AG	-	$0.038{\pm}0.003^{d_1}$	$0.037{\pm}0.005^{b_2 c_2}$

AHH (pmole/min/mg protein)			
Groups	2nd week	10th week	22nd week
Control	11.54±1.17	11.10±1.18	14.68±4.15
Aq.Tc	11.40±1.76	11.59±1.86	11.59±2.17
AG	11.23±1.81	11.80±2.27	15.02±3.50
B(a)P	-	$35.0{\pm}0.69^{a_1 b_1 c_1}$	$39.87{\pm}8.70^{a_1 b_1 c_1}$
B(a)P +Aq.Tc	-	$26.32{\pm}3.26^{d_1}$	$15.15{\pm}3.10^{d_1}$
B(a)P+AG	-	$18.58{\pm}1.80^{d_1 e_1}$	$25.39{\pm}6.33^{a_2 b_1 c_3 d_3 e_2}$

GST (µmole/min/mg protein)			
Group	2nd week	10th week	22nd week
Control	0.135±0.003	0.145±0.008	0.319±0.022
Aq.Tc	0.142±0.004	0.143±0.006	$0.444{\pm}0.013^{a_2}$
AG	0.143±0.004	0.146±0.007	$0.432{\pm}0.083^{a_2}$
B(a)P	-	$0.090{\pm}0.007^{a_1 b_1 c_1}$	$0.823{\pm}0.110^{a_1 b_1 c_1}$
B(a)P +Aq.Tc	-	$0.132{\pm}0.008^{d_1}$	$0.424{\pm}0.048^{d_1}$
B(a)P+AG	-	$0.114{\pm}0.008^{d_1}$	$0.566{\pm}0.020^{a_1 b_2 c_2 d_1 e_2}$

UDP-GT (µmole/min/mg protein)			
Groups	2nd week	10th week	22nd week
Control	19.01±1.02	30.13±2.31	17.09±0.805
Aq.Tc	18.50±1.10	26.70±2.81	16.74±2.030
AG	18.33±0.89	29.79±1.74	17.41±0.883
B(a)P	-	$80.83{\pm}1.98^{a_1 b_1 c_1}$	$12.63{\pm}2.269^{a_2 b_2 c_2}$
B(a)P+ Aq.Tc	-	$31.54{\pm}2.13^{d_1}$	$24.70{\pm}3.554^{a_1 b_1 c_2 d_1}$
B(a)P+AG	-	$33.17{\pm}2.91^{d_1}$	$14.38{\pm}2.471^{d_1}$

[Values are expressed as: Mean $\pm$ SD (n=6) and analysed using one-way ANOVA followed by least significant difference (LSD) post-hoc test. a_1: $P \le 0.001$; a_2: $P \le 0.01$; a_3: $P \le 0.05$ significant as compared to the control group, b_1: $P \le 0.001$; b_2: $P \le 0.01$; b_3: $P \le 0.05$ significant as compared to Aq.Tc group, c_1: $P \le 0.001$; c_2: $P \le 0.01$; c_3: $P \le 0.05$ significant as compared to AG group, d_1: $P \le 0.001$; d_2: $P \le 0.01$; d_3: $P \le 0.05$ significant as compared to B(a)P group, e_1: $P \le 0.001$; e_2: $P \le 0.01$ significant as compared to B(a)P+Aq.Tc group]

Phase II carcinogen metabolising enzymes

Glutathione-S-transferase

After 10th week of the study, significant decrease in the activity of GST was observed in B(a)P treated animals in comparison to control ($P \le 0.01$), Aq.Tc ($P \le 0.01$) and AG ($P \le 0.001$) group, respectively. B(a)P+AG and B(a)P+ Aq.Tc group animals showed significant increase in the GST activity in comparison to the B(a)P ($P \le 0.01$) group. Similarly, at 22nd week, B(a)P treatment resulted in significant increase in the GST activity as compared to control ($P \le 0.001$) and AG group ($P \le 0.001$), whereas, co-administration of AG and Aq.Tc to B(a)P group animals significantly helped to decrease the GST activity in comparison to B(a)P group ($P \le 0.01$) (Table 2).

Uridine diphosphate glucourynyl transferase

After 10th week of the study, significant increase in the activity of UDP-GT was observed in B(a)P treated animals in comparison to control ($P \le 0.01$), Aq.Tc ($P \le 0.01$) and AG ($P \le 0.001$) group, respectively. B(a)P+AG and B(a)P+ Aq.Tc group animals showed significant decrease in the UDP-GT activity in comparison to the B(a)P ($P \le 0.01$) group. Similarly, at 22nd week, B(a)P treatment resulted in significant increase in the UDP-GT activity as compared to control ($P \le 0.001$) and AG group ($P \le 0.001$), whereas, co-administration of AG and Aq.Tc to B(a)P group animals significantly helped to decrease the UDP-GT activity in comparison to B(a)P group ($P \le 0.01$). The UDP-GT activity was significantly lower in B(a)P+AG group when compared to the B(a)P +Aq.Tc ($P \le 0.001$) group (Table 2).

Oxidative stress

Reduced glutathione

After 10th week of the study, significant decrease in the GSH levels were observed in B(a)P treated animals in comparison to control ($P \le 0.01$), Aq.Tc ($P \le 0.01$) and AG ($P \le 0.001$) group, respectively. B(a)P+AG and B(a)P+ Aq.Tc group animals showed significant increase in the GSH levels in comparison to the B(a)P ($P \le 0.001$) group. However, at 22nd week, a significant increase in GSH levels was observed in Aq.Tc and AG group when compared with control ($P \le 0.001$) group. B(a)P treatment resulted in significant decrease in GSH levels as compared to Aq.Tc ($P \le 0.01$) group, whereas, co-administration of AG and Aq.Tc to B(a)P group animals significantly helped to increase the GSH levels in comparison to B(a)P group ($P \le 0.01$) (Table 3).

Lipid peroxidation

After 10th week of the study, significant increase in the LPO levels were observed in B(a)P group when compared with control ($P \leq 0.01$), Aq.Tc ($P \leq 0.01$) and AG ($P \leq 0.01$) group. B(a)P+AG and B(a)P+ Aq.Tc group animals showed significant decrease in the LPO levels in comparison to the B(a)P ($P \leq 0.01$) group. However, at 22nd week, a significant increase

Table 3 — Modulatory effect of Aq.Tc, AG and/or B(a)P on GSH and LPO levels in pulmonary tissue at 2nd, 10th and 22nd week during lung carcinogenesis

	GSH (nmole/mg protein)		
Group	2nd week	10th week	22nd week
Control	5.02±0.67	16.25±1.26	4.53±1.03
Aq.Tc	6.20±0.45	19.65±0.90	6.51±1.11^{a_2}
AG	4.99±0.67	19.55±0.76	4.03±1.37^{b_2}
B(a)P	-	14.34±1.35^{a_1b_1c_1}	3.12±0.97^{b_1}
B(a)P+Aq.Tc	-	17.54±0.122^{d_2}	5.32±1.018^{d_2}
B(a)P+AG	-	16.85±0.570^{d_2}	3.79±1.10^{b_2}
	LPO (nmole/mg protein)		
Groups	2nd week	10th week	22nd week
Control	0.213±0.056	0.248±0.095	0.316±0.036
Aq.Tc	0.217±0.078	0.383±0.061	0.312±0.035
AG	0.200±0.043	0.400±0.060	0.328±0.013
B(a)P	-	1.390±0.133^{a_1b_1c_1}	0.438±0.038^{a_1b_2c_2}
B(a)P+ Aq.Tc	-	0.514±0.103^{a_2d_1}	0.380±0.061^{b_3d_1}
B(a)P+AG	-	0.858±0.101^{a_1b_1c_1d_1e_1}	0.390±0.040^{a_1b_1c_2}

[Values are expressed as: Mean ± SD (n=6) and analysed using one-way ANOVA followed by least significant difference (LSD) post-hoc test. a_1: $P \leq 0.001$; a_2: $P \leq 0.01$ significant as compared to the control group, b_1: $P \leq 0.001$; b_2: $P \leq 0.01$; b_3: $P \leq 0.05$ significant as compared to Aq.Tc group, c_1: $P \leq 0.001$; c_2: $P \leq 0.01$ significant as compared to AG group, d_1: $P \leq 0.001$; d_2: $P \leq 0.01$ significant as compared to B(a)P group, e_1: $P \leq 0.001$ significant as compared to B(a)P + Aq.Tc group]

in LPO levels was observed in B(a)P group when compared to control ($P \leq 0.01$), Aq.Tc ($P \leq 0.001$) and AG ($P \leq 0.001$) group respectively. A significant decrease in LPO levels were observed in B(a)P+ Aq.Tc group when compared with B(a)P ($P \leq 0.01$) group (Table 3).

Genotoxicity study

Chromosomal aberrations

Chromosomes were observed for presence of fragments, pulverization, single and multiple breaks and these aberrations were analysed quantitatively. Chromosome aberration analysis revealed a normal set of 2n= 40 chromosomes with minimum aberrations in control group (Fig. 1). However, B(a)P treatment resulted in pulverization, breaks and various abnormal rearrangements in chromosomes of B(a)P and B(a)P + AG. B(a)P treatment also led to the significant increase in the incidence of aberrant cells in the lungs as compared to control mice ($P \leq 0.01$). Pre-treatment with Aq.Tc significantly decrease the incidence of aberrant cells and abnormalities when compared to B(a)P group ($P \leq 0.01$). Also, reduced DNA strand breaks were observed in B(a)P+AG and B(a)P + Aq.Tc group when compared to B(a)P group (Table 4).

Micronucleus test

The effect of B(a)P on the extent of MN formation was studied and a significant increase in the percentage of MN cells was observed in B(a)P group when compared to control ($P \leq 0.01$), Aq.Tc ($P \leq 0.01$) and AG ($P \leq 0.01$) supplemented group. Moreover, a significant decrease in MN cells were found in both
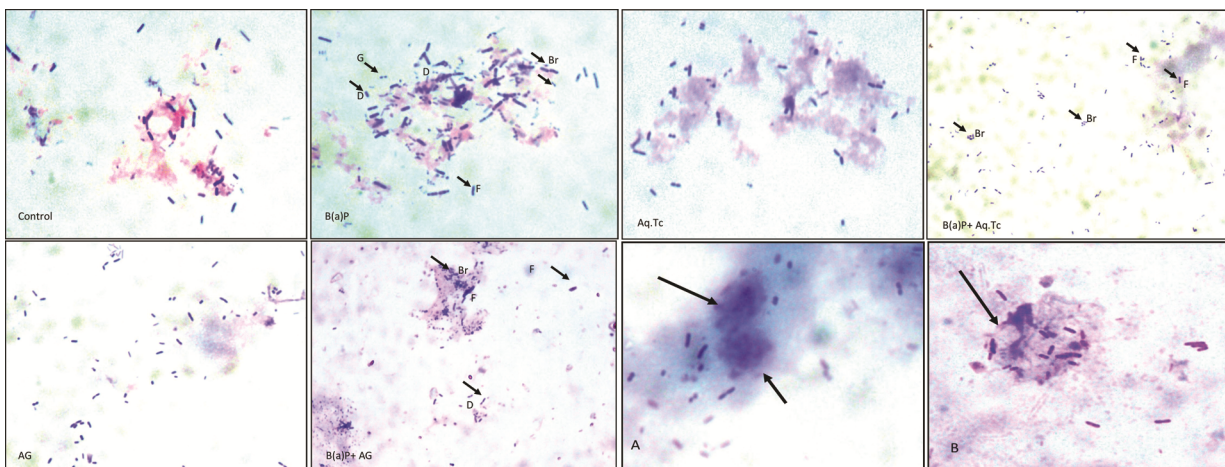

Fig. 1 — Modulatory effect of Aq.Tc and AG on chromosomal aberration analysis after 22 weeks of treatment in different groups. (A) Representative photomicrograph of mouse chromosome showing unburst dividing cell; (B) mouse chromosome showing half burst cell. [GA**:** Gaps, FL: Fragments, Br: Breaks, DL: Deletions]

Table 4 — Semi-quantitative analysis of chromosomal abnormalities in different treatment groups

Groups	Pulverization			Breaks		Incidence of Aberrant cells (%) (Mean ± SD)
	Mild	Moderate	Extensive	Single	Multiple	
Control	+	-	-	+	-	2.0±0.080
Aq.Tc	+	-	-	+	-	1.92±0.042
AG	+	-	-	+	-	2.08±0.049
B(a)P	+	++	++++	+	++++	$16.86\pm1.108a_1b_1c_1$
B(a)P + Aq.Tc	+	++	-	+	-	$5.10\pm0.148a_1b_1c_1d_2$
B(a)P + AG	+	++	++++	+	++++	$11.38\pm1.231a_1b_1c_1d_2e_2$

[(+) Mild pulverization and Single breaks; (-) Absence of pulverization and breaks; (++) Moderate pulverization; (++++) Extensive pulverization and multiple breaks. Data is represented as Mean ± S.D. and analysed using one-way ANOVA followed by least significant difference (LSD) post-hoc test. a_1 represents a significant difference in relation to the control group ($p \leq 0.01$), b_1 represents a significant difference in relation to the Aq.Tc group ($P \leq 0.01$), c_1 represents a significant difference in relation to the AG group ($P \leq 0.01$), d_2 represents a significant difference in relation to the B(a)P group ($P \leq 0.001$), e_2 represents a significant difference in relation to the B(a)P+Aq.Tc group ($P \leq 0.001$)]

B(a)P+AG and B(a)P + Aq.Tc group when compared to B(a)P ($P \leq 0.01$) group. A significant higher percentage of MN cells was observed in B(a)P+AG group when compared with B(a)P + Aq.Tc ($P \leq 0.01$) group (Fig. 2). No significant change in percentage of MN cells was observed in Aq.Tc and AG group when compared with B(a)P group.

Molecular analysis (FT-IR)

Fig. 3 shows mean FTIR spectra of lung tissue/lung tumors from different treatment groups in the (800-4000) cm⁻¹ frequency range. The spectra contained regions associated with characteristics bands of various cellular constituents. The (500-1800) cm⁻¹ region showed characteristic bands of nucleic acids, proteins and carbohydrates.

Phospholipids

The (2800-3050) cm⁻¹ region showed characteristic bands of phospholipids. The mean unsaturation level of phospholipids was measured as $\upsilon=(CH): \upsilon_{as}(CH_3)$; and mean saturation level was measured as $\upsilon_{as}(CH_2): \upsilon_{as}(CH_3)$. and it was found to be significantly decreased in the B(a)P group when compared to control ($P \leq 0.01$), Aq.Tc (p ≤ 0.01) and AG ($P \leq 0.01$) group, respectively. Conversely, the mean unsaturation levels were found to be increased in B(a)P group when compared to control ($P \leq 0.01$), Aq.Tc ($P \leq 0.01$) and AG ($P \leq 0.01$) group. However, tumors treated with Aq.Tc and AG had significantly increased saturation levels of phospholipids and decreased unsaturation levels when compared with the B(a)P group ($P \leq 0.01$), ($P \leq 0.05$) (Table 5).

Glycogen

The relative glycogen content was estimated by calculating the ratio of peak area under curve obtained at (859-1086) cm⁻¹ to peak area at (1520-1550) cm⁻¹.
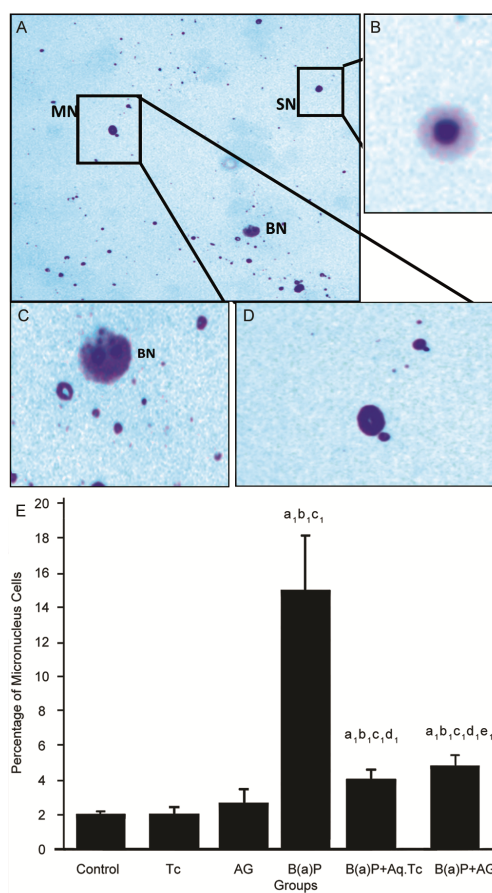

Fig. 2 — Modulatory effect of Aq.Tc and AG on the extent of micronucleus formation after 22 weeks of treatment. (A) Micronucleus formation in B(a)P group; (B) Single nucleated cell (SN); (C) Binucleated cell (BN); (D) Micronucleated cell (MN); and (E) Attenuation in percentage of MN cells in B(a)P induced lung tumors and its chemoprevention by Aq.Tc and AG. [Data is represented as Mean ± S.D. (n= 5) and analysed using one-way ANOVA followed by least significant difference (LSD) post-hoc test. a_1 $P \leq 0.001$ significant with respect to control group; b_1 $P \leq 0.001$ significant with respect to Aq.Tc group; c_1 $P \leq 0.001$ significant with respect to AG group; d_1 $P \leq 0.001$ significant with respect to B(a)P group; e_1 $P \leq 0.001$ significant with respect to B(a)P+ Aq.Tc group]
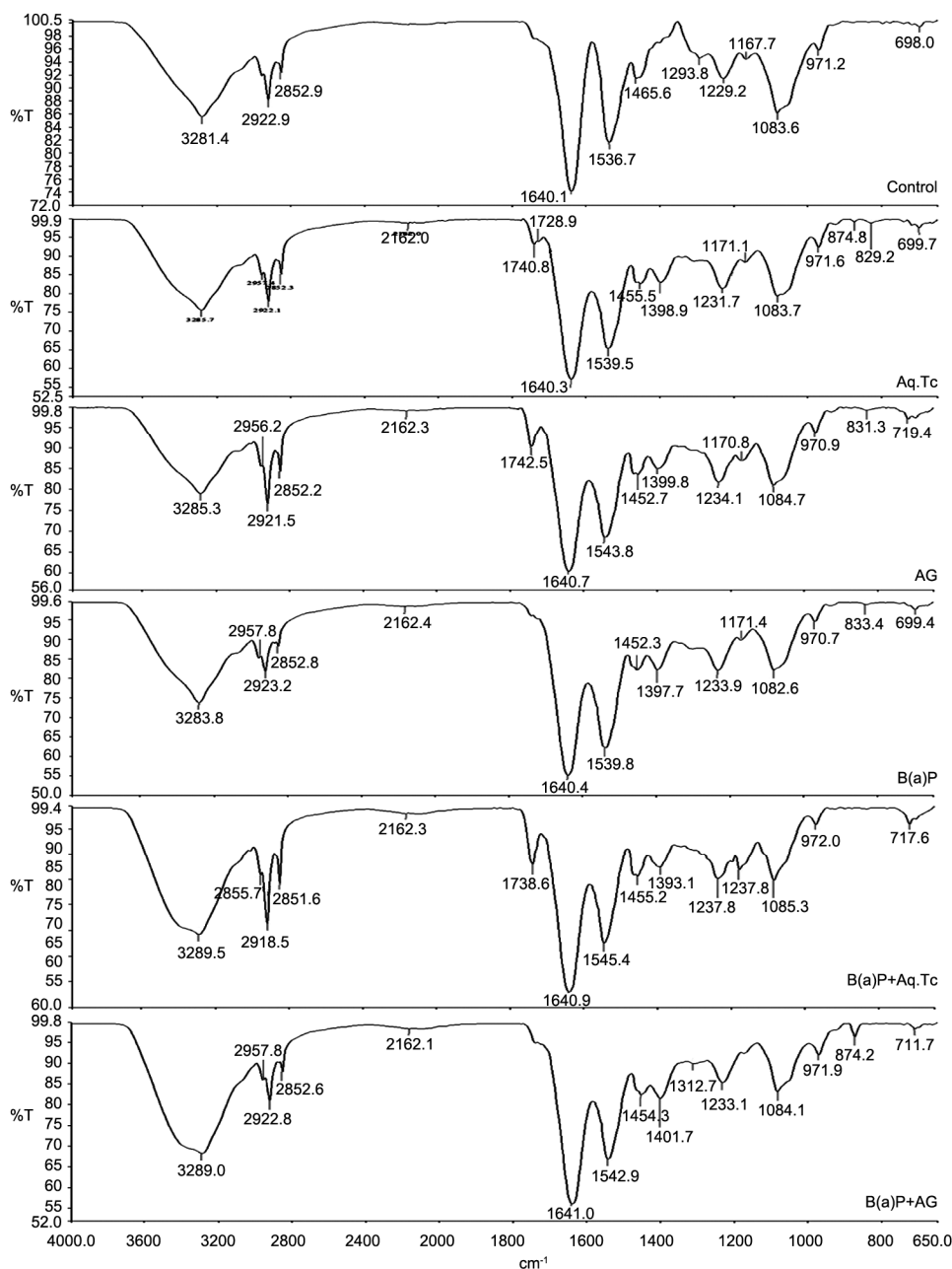
Fig. 3 — FTIR spectrum of lung/lung tumors of mice. [Mean FTIR spectra of each treatment group are displayed in stacked mode]

The peak area under the region of (859-1086) cm^{-1} arises due to C-O stretching band of glycogen coupled with C-O band of C-OH groups. Pulmonary tumors of the B(a)P, B(a)P+ Aq.Tc and B(a)P+AG group showed significantly decreased glycogen levels compared with pulmonary tissue of control ($P \leq 0.01$), Aq.Tc ($P \leq 0.01$) and AG ($P \leq 0.01$) group, respectively. However, these levels were increased in B(a)P + Aq.Tc and B(a)P + AG supplemented group compared with B(a)P group (Table 5).

Nucleic acid

Nucleic acid content was measured by taking a ratio of peak area under (1220-1250) cm^{-1} and (1520-1550) cm^{-1}. The region (1220-1250) cm^{-1} corresponds to asymmetrical phosphate stretching of nucleic acid. Relative nucleic acid content was found to be significantly higher in B(a)P group when compared with control ($P \leq 0.01$), Aq.Tc ($P \leq 0.01$) and AG ($P \leq 0.01$) group, respectively. Moreover, co-supplementation of Aq.Tc and AG to B(a)P treated group significantly decreased glycogen levels to

Table 5 — Effect of Aq.Tc and AG on protein secondary structures, phospholipids, relative glycogen and nucleic acid content in lung/lung tumors

Groups	Secondary Structures			
	α helices	β sheets	Turns	Random coils
Control	14.57±0.261	38.20±0.422	27.20±0.120	25.20±0.310
Aq.Tc	15.08±0.264	38.10±0.366	26.20±0.220	24.70±0.330
AG	14.64±0.46	38.00±0.427	27.60±0.014	25.20 ± 0.210^{a_1b_1}
B(a)P	$23.34\pm0.534^{a_1b_1c_1}$	37.00±0.354	17.07±0.160	$30.60\pm0.230^{a_1b_1c_1}$
B(a)P+Aq.Tc	$13.49\pm0.588^{a_1b_1c_1d_1}$	37.01±0.361	$21.20\pm0.12^{a_1b_1c_1d_1}$	$26.40\pm0.320^{a_1b_1c_1d_1}$
B(a)P+AG	$22.48\pm0.558^{a_1b_1c_1d_2e_1}$	38.10±0.412	$19.61\pm0.230^{a_1b_1c_1d_2}$	$15.10\pm0.120^{a_1b_1c_1d_2}$
Groups	CH/CH$_3$	CH$_2$/CH$_3$	Relative Glycogen content	Relative nucleic acid content
Control	0.613±0.04	10.10±0.32	0.017±0.0004	0.747±0.04
Aq.Tc	0.590±0.03	9.80±0.57	0.015 ± 0.0008^{a_1}	0.733±0.03
AG	0.595±0.03	10.0±0.11	0.014 ± 0.0001^{a_1}	0.693±0.02
B(a)P	0.800 ± 0.01^{a_1b_1c_1}	8.84 ± 0.24^{a_1b_1c_1}	$0.001\pm0.0001^{a_1b_1c_1}$	3.060 ± 0.07^{a_1b_1c_1}
B(a)P+Aq.Tc	0.594 ± 0.02^{d_1}	10.32 ± 0.70^{d_1}	$0.003\pm0.0005^{a_1b_1c_1}$	$0.930\pm0.06^{a_1b_1c_1d_1}$
B(a)P+AG	$0.790\pm0.02^{a_1b_1c_1e_1}$	9.63 ± 0.51^{d_2e_3}	$0.002\pm0.0003^{a_1b_1c_1}$	$1.010\pm0.03^{a_1b_1c_1d_1e_3}$

[Values are expressed as: Mean $\pm$ SD (n=6) and analysed using one-way ANOVA followed by least significant difference (LSD) post-hoc test. a_1: $P \leq 0.001$; a_2: p ≤ 0.01; a_3: $P \leq 0.05$ significant as compared to the control group, b_1: $P \leq 0.001$; b_2: $P \leq 0.01$; b_3: $P \leq 0.05$ significant as compared to Aq.Tc group, c_1: $P \leq 0.001$; c_2: $P \leq 0.01$; c_3: $P \leq 0.05$ significant as compared to AG group, d_1: $P \leq 0.001$; d_2: $P \leq 0.01$; d_3: $P \leq 0.05$ significant as compared to B(a)P group, e_1: $P \leq 0.001$; e_3: $P \leq 0.05$ significant as compared to B(a)P+Aq.Tc group]

normal values when compared with B(a)P group ($P \leq 0.01$), ($P \leq 0.05$) (Table 5).

Protein Secondary structures

Detailed information about the secondary structure of proteins present in lung tissue and tumor tissue was obtained for the analysis of amide I and amide II band (Table 5).

α helices

At the end of 22 weeks, a significant increase in α helical structures were observed in the B(a)P treated group when compared to compared to control ($P \leq 0.01$), Aq.Tc ($P \leq 0.01$) and AG ($P \leq 0.01$) group, respectively. However, Aq.Tc administration significantly reduced the amount to normal levels in B(a)P+ Aq.Tc group when compared to B(a)P group. Also, there was a significant decrease in the same in B(a)P + AG group when compared to B(a)P group but not to normal values as in B(a)P + Aq.Tc group. No significant change in α helical structure was observed in Aq.Tc and AG group when compared to control.

β sheets

At the end of the treatment period, there was no significant change in the β sheet structures in any of the treatment groups.

Turns

A significant decrease in the turns in B(a)P group was observed when compared to control ($P \leq 0.01$),

Aq.Tc ($P \leq 0.01$) and AG ($P \leq 0.01$) group, respectively. Moreover, Aq.Tc and AG supplementation significantly increased the turns to normal level in tumor bearing animals when compared with B(a)P ($P \leq 0.01$) treatment group. No significant change in turns was observed in Aq.Tc and AG group when compared to control.

Random coils

A significant increase in peak area giving rise to random coils was observed in B(a)P group when compared to control (p≤0.01), Aq.Tc ($P \leq 0.01$) and AG ($P \leq 0.01$) group, respectively. However, Aq.Tc and AG treatment significantly decreased the random coils to normal level in tumor bearing animals when compared with B(a)P ($P \leq 0.01$) treatment group.

Electron microscopic studies
Scanning electron microscopy

Fig 4 and 5 show the topographic view of pulmonary tissue from different treatment groups. Alveoli of control animals showed multifaceted structures that were equal in size for a given lung. Also, small bronchioles were well demarcated containing ciliated and non-ciliated areas. The surface of small bronchioles appeared pebbly (Fig. 4A). Cilia were relatively scarce in the distal bronchioles and had the appearance of bushes scattered in a field. The protrusions observed in the centre of the non-ciliated area showed rugged surfaces with sulci and pits. Similar topographical features of lung tissue were
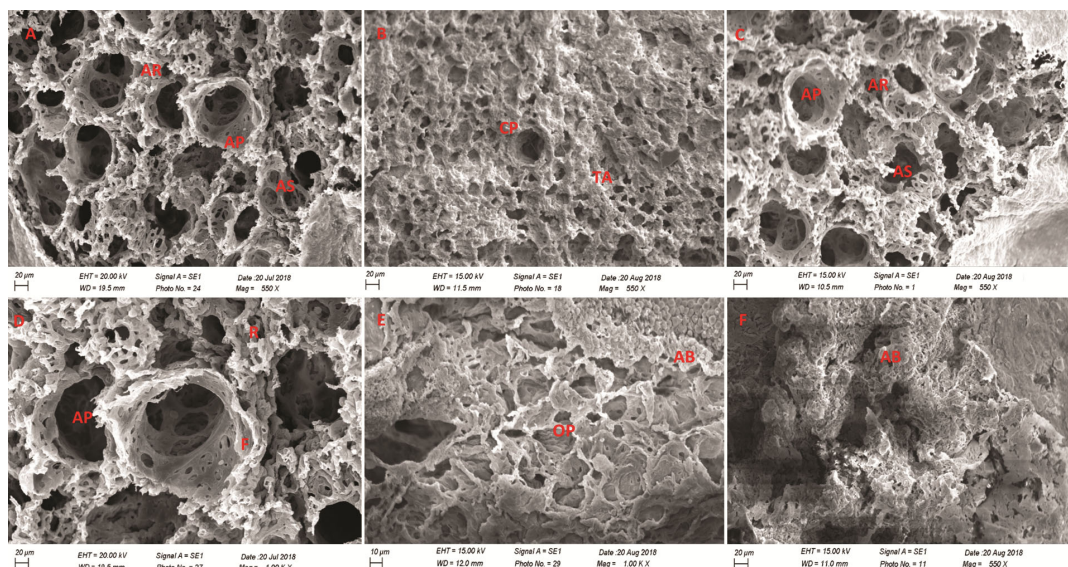
Fig. 4 — Modulatory effect of Aq.Tc and AG on topographic changes in alveolar region of mice lung during B(a)P induced pulmonary carcinogenesis. (A) Control; (B) B(a)P; (C) AqTc; (D) AG; (E) B(a)P+Aq.Tc; and (F) B(a)P+AG group. [AR: Alveolar region; AS: Alveolar sac; AP: Alveolar pore; CP: Constricted pore; TA: Thickened alveolar pore; AB: Apoptotic bodies; OP: Open alveolar duct; F: Fibrous strands; R: many round or ovoid elevation of cells. (Magnification 1000X)]
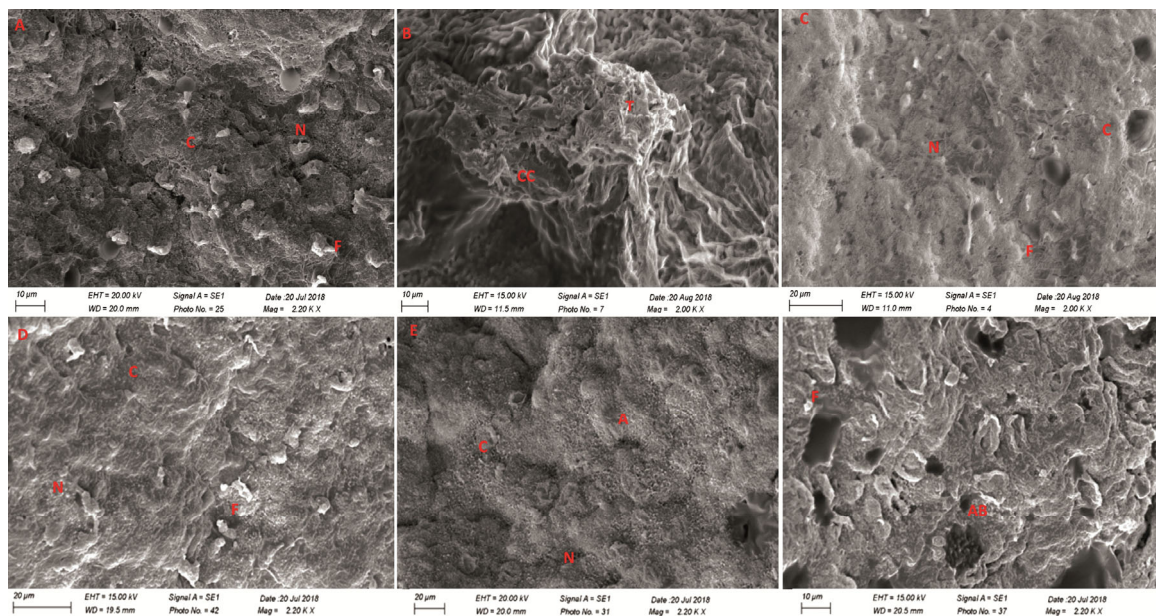

Fig. 5 — Modulatory effect of Aq.Tc and AG on topographic changes in bronchiolar region of mice lung during B(a)P induced pulmonary carcinogenesis (A) Control; (B) B(a)P; (C) AqTc; (D). AG; (E) B(a)P+Aq.Tc; and (F). B(a)P+AG group. [C: Ciliated area N: non-ciliated areas demarcated in a small bronchiole; F: foreign bodies; T: Tumor nodule formation; CC: Clumping of bronchiolar cells; and AB: apoptotic bodies. (Magnification 2200X)]

observed in Aq.Tc and AG treated groups. In lung tumors of the B(a)P treated group, surface disruptions like thickened alveolar epithelium and constricted alveolar pore were visible in the alveolar region. Unlike the normal bronchiolar regions, the SEM of the tumor sections from the B(a)P treated animals

exhibited the tumor nodule formation with clumping of bronchiolar cells (Fig. 4B). However, surface modifications were clearly observed in B(a)P+Aq.Tc animals. Alveolar region appeared normal with intact architecture of cells when compared with B(a)P group. Considering the bronchiolar area of the lung
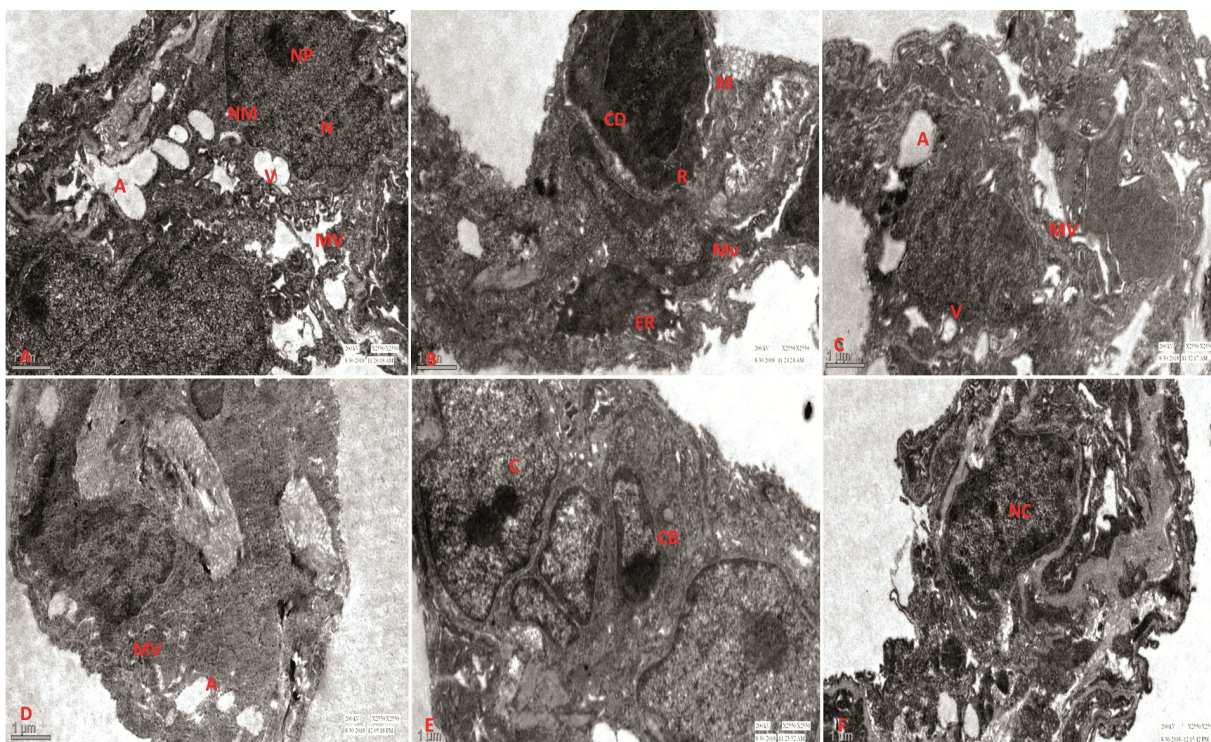
Fig. 6 — Modulatory effect of Aq.Tc and AG on ultrastructure of pulmonary tissue during B(a)P induced lung carcinogenesis. (A) Control; (B) B(a)P group; (C) Aq.Tc group; (D) B(a)P+Aq.Tc group; (E) AG group; and (F) B(a)P+AG group. [A: Alveoli; N: Nucleolus; NP: Nuclear pore; NM: Nuclear membrane; MV: intact microvilli; V: Vacuole; CD: Dense cytoplasm; R: irregular nuclei; M: distorted nuclear membrane; Mv: irregular microvilli; ER: ruptured endoplasmic reticulum, CB: crescent body formation; NC: nuclear clumping and C: chromatin condensation]

very few ciliated and non-ciliated regions were present. In B(a)P+AG treated mice, certain rounded structures were observed that may be the regions of hyper proliferative cells with few apoptotic bodies visible in certain area (Fig. 5).

Transmission electron microscopy

TEM micrographs of lung tissue (Fig. 6) from the control, Aq.Tc and AG treated group showed normal ultra-structural architecture of the cells. TEM studies showed normal nuclear ultra-structure with normal distribution of the chromatin in the nucleoplasm, well defined nucleolus and distinct nuclear membrane. The microvilli on the surface of the alveolar epithelium of the lung seemed to be integral with clean arrangement. Changes in the ultra-structure of the lung cells was evident in the tumors of the animals that received only B(a)P instillations. The nucleus seemed to be irregular in shape along with the disruption in the nuclear membrane. Following exposure of B(a)P, extensive vacuolization in the cytoplasm was also observed. However, Aq.Tc supplementation to B(a)P treated animals resulted in the improvement of ultra-structure of lung cells. Classical feature of apoptosis like chromatin condensation/hyper condensation, nuclear pyknosis and apoptotic bodies were clearly evident. Some cells also showed the presence of cytoplasmic granulation, another feature of apoptosis. Further, AG supplementation to the tumor bearing mice resulted in appreciable improvement in alveolar epithelium and vacuolization of the cells. Nuclear clumping was another feature which was evident in these animals (Fig. 6).

Discussion

Tinospora cordifolia (Tc) is an indigenous medicinal plant having various pharmacological properties making it an ideal drug for testing in cancer protocols. The quality of medicinal plants depends on the quantity of various trace elements present in it and also their consumption may affect the physiological functioning of the human body[23]. Many trace elements have been known to play an important role in the formation of the active constituents present in medicinal plants. Aq.Tc showed the presence of potassium, calcium, magnesium, iron, sulphur, etc. in considerable amounts. Deficiencies/imbalances of these elements may lead to physiological disorders.

Aq.Tc contained high amount of K and Ca and are known to play essential part of body metabolism. Present results were in concordance with other reports available in literature that demonstrated the presence of the above mentioned essential elements in Aq.Tc stem extract[24]. Therefore, it could be inferred from the above observations that Aq.Tc contained essential trace elements and can be considered safe for human or animal consumption.

B(a)P is a known lung carcinogen (pro-carcinogen), activated by phase I biotransformation enzymes i.e., cytP$_{450}$to its ultimate carcinogenic form. Cyt P$_{450}$ metabolizes various xenobiotics to more reactive electrophilic moieties, which in turn are detoxified by phase II enzymes[3]. In the present study, a significant increase of Cyt P$_{450}$ and Cyt b$_5$ activity was observed after B(a)P insult at 10th and 22nd week of the treatment. Induction of phase I enzymes due to the carcinogenic insult signifies the initiation of the carcinogenic process. As it is well known that phase I enzymes perform the activation of pro-carcinogens to active carcinogenic metabolites, which if not detoxified by phase II enzymes may result in the induction of mutations critical for carcinogenesis[25]. Our findings were in concordance with previous studies, which demonstrated an increase in phase I metabolising enzymes in B(a)P administered animals[26]. AHH is a phase I CME that plays an important role in metabolism of B(a)P. In the present study, induction of AHH enzyme was observed at 10th and 22nd week of the treatment in B(a)P group. However, Aq.Tc and AG pre-treatment to B(a)P group led to the significant decrease in AHH activity in tumor bearing mice which in turn depicts decrease in formation of carcinogenic metabolites and consequently delay in the process of carcinogenesis. Similar results have been reported by other researchers wherein treatment of Tc extract helped in reduction of phase I enzymes[27].

Action of phase II enzymes such as GST and UDPGT is considered to be a major mechanism of protection against chemical stress and inhibition of carcinogenesis. GST catalyses the conjugation of reactive chemicals with GSH and subsequently eliminate it via a GSH conjugate-recognizing transport[28]. A significant decrease in GST activity was observed at 10th week of the treatment in B(a)P group. Reports available in the literature suggest a relationship between the depletion of GST and an increase in cancer susceptibility. A concomitant increase in GST activity upon AG and Aq.Tc supplementation in B(a)P animals depicts their role in increasing the ability of cells to detoxify activated metabolic products of B(a)P by upregulating the activity of phase II enzymes. Earlier reports from literature also support our observation which showed that administration of water-soluble polysaccharide from *Antrodia cinnamomea* significantly increased the GST activity in liver cells[29].

B(a)P isa powerful carcinogen with a capability to induce enormous amounts of free radicals, which in turn reacts with lipids causing lipid peroxidation. In the present study, increased LPO in B(a)P group may be due to the excessive free radicals produced by administration of B(a)P. LPO leads to the formation of several toxic products such as malondialdehydes which can attack cellular targets, thereby modulating various signalling pathways associated with cellular proliferation and apoptosis[30]. In our previous study, increased apoptosis was observed in B(a)P group which could be correlated to the increased LPO levels in this group. Significantly depleted levels of LPO was observed in B(a)P+Aq.Tc and B(a)P +AG group. This clearly shows that Aq.Tc and AG inhibits LPO thereby limiting the formation of free radicals which are involved in carcinogenesis.

GSH is a non-enzymatic antioxidant that plays a vital role in detoxification of xenobiotic compounds, reactive oxygen species and free radicals[31]. Present study showed a significant decline in GSH levels in B(a)P group, which may be due to excessive utilization of antioxidants in tumor cell proliferation or the ROS-mediated damage at the initiation as well as progression phase of tumorigenesis. However, increased GSH levels were found in B(a)P + AG group at 10th and 22nd week which also suggests the free radical scavenging ability of AG. Furthermore, enhanced GSH levels were found in B(a)P + Aq.Tc group which suggests the better antioxidant capacity of Tc plant extract to combat oxidative stress imposed by B(a)P. The elevated level of GSH induced by Tc protects cellular proteins against oxidation (via GSH redox cycle) and also directly detoxifies reactive intermediate species generated from exposure to B(a)P. Similar findings have been reported earlier in which supplementation of chemopreventive agents elevated the levels of GSH in cancer bearing mice[32]. The depletion of GSH below its optimum level induces oxidative stress

with a cascade of events leading to malfunctioning of structural integrity of cells and organelle membranes.

A variety of genotoxic agents or carcinogens are known to induce MN formation leading to cell death, genomic instability, or cancer development. In the present study, significantly higher percentage of MN cells in B(a)P group revealed the genotoxic effect in pulmonary tissue. Other reports in various experimental models divulged a similar increased MN formation upon B(a)P instillation[33].However, pre-treatment of Aq.Tc and AG to B(a)P challenged animals showed decreased level of pulmonary MN cells in the present study suggesting an antigenotoxic effect of both the agents. AG is a natural PS and has shown to reduce MN cells in liver, lung as well as bone marrow of tumor bearing animals[34].Chromosomal abnormalities have been found to affect various pre-neoplastic and neoplastic lesions which are further involved in the progression of carcinogenesis. These abnormalities play an important role in the activation of oncogenes and inactivation of tumor suppressor genes, indicating the usefulness of such cytogenetic studies in carcinogenesis. Increased chromosomal damage was apparent in B(a)P group as observed by higher number of fragments and deletions in the chromosomes. Moreover, Aq.Tc and AG supplementation to B(a)P group resulted in decrease in total percentage of aberrant cells and also helped in reduction of chromosomal breaks and distortions. Chromosomal and micronucleus assay indicated that Aq.Tc and AG supressed the clastogenic effect of B(a)P and hence is involved in the delay of the progression or development of pulmonary tumors.

Carcinogenesis leads to alterations of biomolecules which include an increase in disorder of the membrane lipids, disruption in protein structures and changes in the biochemical composition of cells[35]. In the present study, decreased saturation levels in phospholipids of B(a)P-induced tumors indicate severe changes during pulmonary carcinogenesis. The fluidity of the plasma membrane is largely dependent upon lipid content and the extent of saturation in fatty acyl chains. A decrease in saturation level of fatty acyl chains in the tumor cells increases the fluidity in the plasma membrane[36]. It has also been documented that lesser fluidity in the plasma membrane may have an inhibitory effect on cell growth, thereby delaying carcinogenesis. The normalization of mean saturation

levels in B(a)P + Aq.Tc group thus indicates decreased fluidity of the plasma membrane compared with B(a)P-induced tumors, and this activity might be responsible for its anticancer action. Similar reports have been demonstrated by other researchers in which administration of plant extracts affected the membrane fluidity as well as lipid composition in tumor bearing mice[37]. Also, AG administration restored the mean saturated and unsaturated phospholipid composition in B(a)P treated animals. In the present study, protein secondary structures were evaluated in terms of percentage of α helices, β sheets, turns, and random coils. B(a)P treatment resulted in the increased the amount of α helices and random coils; whereas turns were found to be decreased in these animals. These changes in the secondary structure may indicate some important structural alterations in the existing proteins or the expression of new types of proteins occurring under the tumor transformation. Present results are in line with the available literature which showed similar changes in the protein secondary structures in DMBA- induced hamster buccal pouch carcinogenesis. On the other hand, Aq.Tc and AG supplementation restored the amount of α helices, β sheets, turns, and random coils indicating the ability of Aq.Tc and AG to suppress carcinogenesis by modulating cellular transformation and controlling cell proliferation and differentiation.

In addition, FT-IR spectra also revealed changes in the glycogen content of lung tissue in various treatment groups. The decrease of relative amount of glycogen in pulmonary tissue of B(a)P treated animals depict increased glucose consumption in tumor cells. Cancer cells are well known to use glycogen at a much higher rate than normal cells to meet their energy requirements[38]. However, Aq.Tc and AG supplementation to B(a)P treated animals significantly increased the glycogen levels showing that treatment inhibited the microevolution of pulmonary cancer cells and provided protection against carcinogenesis. Similar results have been demonstrated earlier regarding the increase in glycogen levels in lung carcinoma cells. Also a significant increase in relative nucleic acid content (RNA and DNA) of B(a)P treated pulmonary tissue depicting increased cellular proliferation in these animals. These changes may reflect an increase in mitotic index of cells or elevated RNA content due to upregulation of certain genes in

the cell. Moreover, Aq. Tc and AG treatment to cancer bearing animal reduce the levels of nucleic acid drastically depicting delay in carcinogenic process. The altered molecular composition is a vital parameter of carcinogenic transformation; thus, by modulating molecular status of cancer cells, Aq. Tc and AG may have delayed the process of evolution and growth of lung tumors.

The process of carcinogenesis may lead to formation of a transformed cell involving various topographical and ultrastructural changes. SEM studies of pulmonary tissue from B(a)P group showed loss of alveolar arrangement as well as constriction of the bronchiolar pore. In addition, tumor nodule formation with clumping of bronchiolar cells was evident. However, treatment of Aq.Tc and AG to cancer bearing animals normalized these changes along with the appearance of apoptotic bodies. TEM studies of lung tissue from B(a)P group revealed phaeomorphic cells, alveolar damages and more number of pyknotic nuclei. Further, the alveolar damage was accompanied by increased number of hyperchromatic, irregular nuclei in the alveolar cells. Number of organelle present in a cell is directly proportional to its degree of differentiation. It is well documented that the amount of organelle has the tendency to decline when differentiation declines[39]. B(a)P treatment to mice resulted in overall rarefaction of cytoplasm, indicating decreased level of differentiation in these cells. Similar results have been demonstrated by other researchers wherein B(a)P resulted in loss of ultrastructure of pulmonary tissue[40]. Pronounced tumor progression observed in the B(a)P-induced mice might be due to enormous proliferation of the aberrant cancer cells. Aq.Tc and AG treatment showed early and late apoptosis characterised by the presence of irregular and fragmented nuclei, shrunken cells and clumping/alterations in mitochondria.

Conclusion

In our earlier studies, we reported that Aq. Tc and AG was effective in mitigating B(a)P induced lung tumorigenesis. The delay in carcinogenesis was demonstrated through histopathological alterations, improved tumor markers and reduced tumor burden. In the present study, we have extended this work to gain insights about the *in vivo* anticancer activity of

Aq.Tc and AG in lung tumorigenesis on the basis of various biochemical, molecular and ultrastructural changes. The results of the present study revealed that Aq.Tc and AG modulated key processes like carcinogen biotransformation enzymes and ROS generation during B(a)P induced lung carcinogenesis. This therapeutic potential was further dictated by the mitigation of clastogenic damages as well as preserved cellular architecture of pulmonary tissue suggesting the antigenotoxic effects of both Aq. Tc and AG. FT-IR analysis was carried out to investigate the alterations in composition of biomolecules of pulmonary tumors. Aq.Tc and AG supplementation restored molecular composition in lung tumors indicating the ability of Aq.Tc and AG to suppress carcinogenesis by hampering the process of evolution of tumors. These medicinal properties of Tc may be credited to the synergistic effects of different phyto-constituents present in it. However, additional studies are required to explore the other protective mechanisms and to recommend *Tinospora cordifolia* as an effective chemopreventive agent.

Conflict of interest

Authors declare no competing interests.

References

1   Sung H, Ferlay J, Siegel RL, Laversanne M, Soerjomataram I, Jemal A & Bray F, Global cancer statistics 2020: GLOBOCAN estimates of incidence and mortality worldwide for 36 cancers in 185 countries. *CA Cancer J Clin*, 71 (3) (2021) 209. https://doi.org/10.3322/caac.21660.

2   Barta JA, Powell CA & Wisnivesky JP, Global epidemiology of lung cancer. *Ann Glob Health*, 85 (2019) 8.

3   Velli SK, Sundaram J, Murugan M, Balaraman G & Thiruvengadam D, Protective effect of vanillic acid against benzo(a)pyrene induced lung cancer in swiss albino mice. *J Biochem Mol Toxicol*, 33 (2019) 1.

4   Piberger AL, Kruger CT, Strauch BM, Schneider B & Hartwig A, BPDE-induced genotoxicity: relationship between DNA adducts, mutagenicity in the *in vitro* PIG-A assay, and the transcriptional response to DNA damage in TK6 cells. *Arch Toxicol,*, 92 (2018) 541.

5   Paolillo M & Schinelli S, Extracellular alterations in metastatic processes. *Int J Mol Sci*, 20 (2019) 4947.

6   Peixoto A, Relvas-Santos M, Azevedo R, Santos LL & Ferreira JA, Protein glycosylation and tumor microenvironment alterations driving cancer hallmarks. *Front Oncol*, 9 (2019) 380.

7   Singh D & Chaudhuri PK, Chemistry and pharmacology of *Tinospora cordifolia*. *Nat Prod Commun*, 12 (2017) 299.

8   Leyon PV & Kuttan G, Inhibitory effect of a polysaccharide from *Tinospora cordifolia* on experimental metastasis. *J Ethnopharmacol*, 90 (2004) 233.

9   Pandey VK, Shankar BS & Sainis KB, G1-4A, an arabinogalactan polysaccharide from *Tinospora cordifolia* increases dendritic cell immunogenicity in a murine lymphoma model. *Int Immunopharmacol*, 14 (2012) 641.

10 Mohan V & Koul A, Anticancer potential of *Tinospora cordifolia* and arabinogalactan against benzo(a)pyrene induced pulmonary tumorigenesis: A study in relevance to various biomarkers. *J HerbMed Pharmacol*, 7 (2018) 225.

11 Koul A, Garg S & Mohan V, Chemopreventive role of arabinogalactan against experimentally induced pulmonary carcinogenesis: a study in relation to its initiation phase. *Drug Chem Toxicol*, 5 (2019) 1.

12 Rajakumar T, Pugalendhi P & Thilagavathi S, Dose response chemopreventive potential of allyl isothiocyanate against 7,12-dimethylbenz(a)anthracene induced mammary carcinogenesis in female Sprague-Dawley rats. *Chem Biol Interact*, 231 (2015) 35.

13 Koul A, Mohan V & Bharati S, *Azadirachta indica* mitigates DMBA-induced hepatotoxicity: A biochemical and radiometric study. *Indian J Biochem Biophys*, 51 (2014) 37.

14 Nebert DW & Gelboin HV, The *in vivo* and *in vitro* induction of aryl hydrocarbon hydroxylase in mammalian cells of different species, tissues, strains, and developmental and hormonal states. *Arch Biochem Biophys*, 134 (1969)76.

15 Devadoss D, Ramar M & Chinnasamy A, Galangin, a dietary flavonol inhibits tumor initiation during experimental pulmonary tumorigenesis by modulating xenobiotic enzymes and antioxidant status. *Arch Pharm Res*,, 41 (2018) 265.

16 Gorski JP & Kasper CB, Purification and properties of microsomal UDP-glucuronosyltransferase from rat liver. *J Biol Chem*, 252 (1977) 1336.

17 Moron MS, Depierre JW & Mannervik B, Levels of glutathione, glutathione reductase and glutathione S-transferase activities in rat lung and liver. *Biochim Biophys Acta*, 582 (1979) 67.

18 Trush MA, Mimnaugh EG, Ginsburg E & Gram TE, *In vitro* stimulation by paraquat of reactive oxygen-mediated lipid peroxidation in rat lung microsomes. *Toxicol Appl Pharmacol*, 60 (1981) 279.

19 Lowry OH, Rosebrough NJ, Farr AL & Randall RJ, Protein measurement with folin-phenol reagent. *J Biol Chem*, 193 (1951) 265.

20 Bala S, Chugh NA, Bansal SC, Garg ML & Koul A, Radiomodulatory effects of Aloe vera on hepatic and renal tissues of X-ray irradiated mice. *Mutat Res*, 811 (2018) 1.

21 Schmid W, The micronucleus test. *Mutat Res*, 31 (1975) 9.

22 Lewis PD, Lewis KE, Ghosal R, Bayliss S, Lloyd AJ, Wills J, Godfrey R, Kloer P & Mur LA, Evaluation of FT-IR spectroscopy as a diagnostic tool for lung cancer using sputum. *BMC Cancer*, 10 (2010) 640.

23 Sium M, Kareru P, Keriko J, Girmay B, Medhanie G & Debretsion S, Profile of trace elements in selected medicinal plants used for the treatment of diabetes in Eritrea. *Sci World J*, 2016 (2016) 2752836.

24 Gowrishankar R, Kumar M, Menon V, Divi SM, Saravanan M, Magudapathy P, Panigrahi BK, Nair KGM & Venkataramaniah K, Trace element studies on *Tinospora cordifolia* (Menispermaceae), *Ocimumsanctum* (Lamiaceae), *Moringa oleifera* (Moringaceae) and *Phyllanthus niruri* (Euphorbiaceae) Using PIXE. *Biol Trace Elem Res*, 133 (2010) 357.

25 Kasala ER, Bodduluru LN, Barua CC, Sriram CS & Gogoi R, Benzo(a)pyrene induced lung cancer: Role of dietary phytochemicals in chemoprevention. *Pharmacol Rep*, 67 (2015) 996.

26 Naveenkumar C, Raghunandakumar S, Asokkumar S, Binuclara J, Rajan B, Premkumar T & Devaki T, Mitigating role of baicalein on lysosomal enzymes and xenobiotic metabolizing enzyme status during lung carcinogenesis of Swiss albino mice induced by benzo(a)pyrene. *Fundam Clin Pharmacol*, 28 (2014) 310.

27 Singh RP, Banerjee S, Kumar PVS, Raveesha KA & Rao AR, *Tinospora cordifolia* induces enzymes of carcinogen/drug metabolism and antioxidant system, and inhibits lipid peroxidation in mice. *Phytomedicine*, 13 (2006) 74.

28 Allocati N, Masulli M, Di-Ilio C & Federici L, Glutathione transferases: substrates, inihibitors and pro-drugs in cancer and neurodegenerative diseases. *Oncogenesis*, 7 (2018) 8.

29 Tsai MC, Song TY, Shih PH & Yen GC, Antioxidant properties of water-soluble polysaccharides from *Antrodia cinnamomea* in submerged culture. *Food Chem*, 2104 (2007) 1115.

30 Ayala A, Munoz MF & Arguelles S, Lipid peroxidation: production, metabolism, and signaling mechanisms of malondialdehyde and 4-hydroxy-2-nonenal. *Oxid Med Cell Longev*, 2014 (2014) 360438.

31 Chodakowska IM, Witkowska AM & Zujko ME, Endogeneous non-enzymatic antioxidants in the human body. *Adv Med Sci*, 63 (2018) 68.

32 Sun J, Wen X, Liu J, Kan J, Qian C, Wu C &Jin C, Protective effect of an arabinogalactan from black soybean against carbon tetrachloride-induced acute liver injury in mice. *Int J Biol Macromol*, 117 (2018) 659.

33 Jahangir T, Safhi MM, Sultana S & Ahmad S, *Pluchea lanceolata* protects against Benzo(a)pyrene induced renal toxicity and loss of DNA integrity. *Interdiscip Toxicol*, 6 (2013) 47.

34 Posocco B, Dreussi E, de Santa J, Toffoli G, Abrami M, Musiani F, Grassi M, Farra R, Tonon F, Grassi G & Dapas B, Polysaccharides for the Delivery of Antitumor Drugs. *Materials*, 8 (2015) 2569.

35 Brozek-Pluska B, Musial J, Kordek R & Abramczyk H, Analysis of human colon by raman spectroscopy and

imaging-elucidation of biochemical changes in carcinogenesis. *Int J Mol Sci*, 20 (2019) 3398.

36 Zalba S & Hagen TLM, Cell membrane modulation as adjuvant in cancer therapy. *Cancer Treat Rev*, 52 (2017) 48.

37 Nandakumar N, Jayaprakash R, Rengarajan T, Ramesh V & Balasubramanian MP, Hesperidin, a natural citrus flavonoglycoside, normalizes lipid peroxidation and membrane bound marker enzymes in 7, 12-Dimethylbenz(a)anthracene induced experimental breast cancer rats. *Biomed Prev Nutr*, 1 (2011) 255.

38 Fadaka A, Ajiboye B, Ojo O, Adewale O, Olayide I & Emuowhochere R, Biology of glucose metabolization in cancer cells. *J Oncol Sci*, 3 (2017) 45.

39 Anandakumar P, Kamaraj S, Jagan S, Ramakrishnan G & Devaki T, Capsaicin provokes apoptosis and restricts benzo(a)pyrene induced lung tumorigenesis in Swiss albino mice. *Int Immunopharmacol*, 17 (2013) 254.

40 Ravichandran N, Suresh G, Ramesh B, Manikandan R, Choi YW & Vijaiyan SG, Fisetin modulates mitochondrial enzymes and apoptotic signals in benzo(a)pyrene-induced lung cancer. *Mol Cell Biochem*, 390 (2014) 225.